# Disappearance and reappearance of above-threshold-ionization peaks

Lars Bojer Madsen
*Department of Physics and Astronomy, Aarhus University, DK-8000 Aarhus C, Denmark*

(Received 12 July 2022; accepted 7 October 2022; published 27 October 2022)

It is shown that above-threshold-ionization peaks disappear when the kinetic energy associated with the nondipole radiation-pressure-induced photoelectron momentum in the laser propagation direction becomes comparable to the photon energy, and how peaks can be made to reappear if knowledge of the length and direction of the photoelectron momentum is at hand and an emission-direction-dependent momentum shift is accounted for. In this sense appropriate analysis of the nondipole effects restores the energy-conserving signature of the above-threshold-ionization peaks. The reported findings should be observable with intense midinfrared laser pulses.

DOI: 10.1103/PhysRevA.106.043118

## I. INTRODUCTION

During the last decade a number of experimental strong-field ionization studies have measured and modeled nondipole effects across near- [1–6] and midinfrared wavelengths [7–10]. The nondipole signatures are typically in terms of a shift in the maximum of the photoelectron momentum distribution (PMD) in the laser propagation direction away from vanishing momentum as would be the expected position of the maximum in the dipole case. Nondipole effects have also been investigated theoretically at near- and midinfrared wavelengths in intense pulses using a combination of strong-field approximation (SFA), time-dependent Schrödinger equation (TDSE), and tunneling approaches; see, e.g., Refs. [11–33]. The breakdown of the electric dipole approximation in this regime has been known for some time and is due to radiation pressure and magnetic-field effects [34–37]. Progress in the study of nondipole effects was recently reviewed [38–40].

In the photoelectric effect, a peak in the photoelectron spectrum shows up at a kinetic energy $k^2/2 = \omega - I_p$, where $\omega$ is the angular frequency of the ionizing light and $I_p$ is one of the ionization potentials (atomic units are used throughout). In multiphoton ionization, multiple peaks in the spectrum may show up as described by $k^2/2 = n\omega - I_p$, for different integers $n$ making the right-hand side positive, a process known as above-threshold ionization (ATI), where an already free electron absorbs photons. If the ionizing radiation is supplied by an intense laser pulse of subpicosecond duration, the ATI spectrum will show peaks at [41,42]

$$k^2/2 = n\omega - I_p - U_p, \tag{1}$$

where the ponderomotive potential, $U_p = F_0^2/(4\omega^2)$, with $F_0$ the field strength, is the cycle-averaged kinetic energy of the free electron in the laser pulse. Finite pulses have finite bandwidths and result in a broadening of the ATI peaks.

It is useful to relate Eq. (1) to the PMD. Let the laser propagate in the $x$ direction and be linearly polarized along the $z$ axis. Consider the PMD in the $(k_x, k_z)$ plane. Equation (1) then expresses that the PMD may attain signal on concentric circles or rings centered at the origin $(k_{x0}, k_{z0}) = (0, 0)$ with radii

$$k^D = \sqrt{2(n\omega - I_p - U_p)}. \tag{2}$$

Very recently, however, an experiment [43] used a dedicated setup with two counterpropagating 800-nm laser pulses to detect a small decrease (increase) in the lengths of the momenta in (opposite) the laser propagation direction. Clearly, this finding contradicts the implications of Eq. (1). No matter how intuitively appealing Eq. (1) is, it is still an approximation. Equation (1) is only accurate within the electric dipole approximation for the description of the light-matter coupling, i.e., when the dependence of the coupling on the laser propagation direction is neglected. Indeed, the small measured shifts in the angle-resolved ATI peaks [43] are in agreement with theory predictions [23,25,28,34] that take effects beyond the electric dipole approximation into account. A further exploration of the implications of these effects is the purpose of the present paper.

## II. THEORY, RESULTS, AND DISCUSSION

When nondipole effects are considered to first order in $1/c$, with $c$ the speed of light, Eq. (1) is replaced by a relation that takes radiation pressure effects into account. In the $(k_x, k_z)$ momentum plane, energy conservation can be expressed as [23,25,28,34]

$$(k_x - U_p/c)^2/2 + k_z^2/2 = n\omega - I_p - U_p. \tag{3}$$

Equation (3) shows that the final momenta are confined to circles with center

$$(k_{x0}, k_{z0}) = (-U_p/c, 0), \tag{4}$$

and radius given in Eq. (2), where in the latter the superscript $D$ indicates that the radius of the ATI ring is as in the dipole case. TDSE simulations at near-infrared wavelengths verified

 

this shift [27] and it is in agreement with experiment [43]. Therefore, the overall character of the nondipole PMD is determined by signal at energy conserving ATI rings, the centers of which are shifted as specified by Eq. (4). As a consequence of the center shift, the length of the final momenta with respect to the origin in the momentum plane becomes angle dependent. Let $\theta$ denote the polar angle measured with respect to the origin and the positive $z$ axis, i.e., the polarization direction. It is then found that energy conservation is fulfilled at the momenta

$$k_x(\theta) = [k^D - U_p \sin(\theta)/c] \sin(\theta), \tag{5}$$

$$k_z(\theta) = [k^D - U_p \sin(\theta)/c] \cos(\theta). \tag{6}$$

The results above are known [28], and the predicted emission-angle-dependent shift in the length of the photoelectron momentum [16,23,25,34] is confirmed by experiment [43], but their implications for intense midinfrared fields have not been fully realized. Here it will be stressed that the possibility of observing characteristic ATI spectra with peaks at the energies of the individual photon absorption channels can be significantly affected by nondipole terms. The possibility of observation of peaks or not depends on the magnitude of the radiation-pressure-induced momentum shift, $-U_p/c$, in the propagation direction. Clearly, when this shift is of the order of the distance between ATI rings, the rings are shifted such that integration over emission angle for fixed magnitude of continuum electron energy or fixed momentum with respect to the origin will not capture the $\boldsymbol{k}$ values where energy conservation is fulfilled in the nondipole treatment, Eq. (3), and the peaks disappear.

A comparison with results including higher-order terms in $1/c$ [16,23,34] shows that Eq. (3) is valid when $k_x/c \ll 1$. In intense circularly polarized fields, $\langle k_x \rangle$ can be estimated by $\sim U_p/c$, and in linearly polarized fields this mean value is typically less [1]. For a conservative estimate of the applicability range of Eq. (3) in terms of laser parameters and for linearly polarized light, $\langle k_x \rangle$ is therefore estimated by $U_p/c$, so the condition for application of Eq. (3) is $(U_p/c)^2 \ll 1$. For a typical strong-field intensity of $10^{14}$ W/cm$^2$, this condition leads to $\omega \gg 2 \times 10^{-4}$ a.u., corresponding to photon energies much larger than 5 meV or wavelengths much shorter than 240 $\mu$m. The laser parameters considered in the examples below fulfill these conditions.

The magnitude of the magnetic nondipole effect under investigation is conveniently quantified by the parameter

$$\beta_0 = U_p/(2\omega c), \tag{7}$$

which describes the amplitude in the laser propagation direction of the nondipole figure-8 motion of the electron [37]. When $\beta_0 \simeq 1$, nondipole effects are expected to appear. An alternative measure is obtained when one compares the magnitude of the difference in radii between two consecutive photon-absorption rings to the momentum shift $U_p/c$. Such reasoning leads to the parameter

$$\beta_1 = 4\nu\left[\left(U_p^2/c^2/2\right)/\omega\right], \tag{8}$$

where the term in the square bracket is the kinetic energy associated with the radiation-pressure-induced photoelectron momentum in the propagation direction in units of the photon energy, and where $\nu = 5, 6, 7, \ldots$ measures the number of photons absorbed above threshold. The values of $\nu$ start at 5 to justify a Taylor expansion necessary for obtaining the result in Eq. (8). When the value of $\beta_1$ becomes of the order of unity significant nondipole effects are expected.

TABLE I. Parameters $\beta_0$ [Eq. (7)] and $\beta_1$ [Eq. (8)] used to assess the importance of nondipole effects for an intensity of $10^{14}$ W/cm$^2$ for the wavelengths considered in Fig. 1.

| Wavelength, $\lambda$ (nm) | $\beta_0$ | $\beta_1$ ($\nu = 5$) |
|---|---|---|
| 1600 | 0.11 | 0.014 |
| 2400 | 0.37 | 0.11 |
| 3200 | 0.90 | 0.46 |
| 6400 | 7.18 | 14.7 |

To first capture qualitatively the impact of nondipole effects on ATI spectra obtained by a pulsed laser in as simple physical terms as possible it suffices to consider a finite top-hat pulse with $N$ cycles each of duration $T = 2\pi/\omega$. The appearance and disappearance of the ATI peak is governed by the intercycle interference term responsible for energy conservation in the long pulse limit; see, e.g., Refs. [44–47] for discussion of such interference within the electric dipole approximation. During each cycle, a phase $e^{in2\pi \frac{E(\boldsymbol{k})}{\omega}}$ is picked up by the outgoing electron with an energy including a nondipole correction that depends on the projection, $k_x$, of $\boldsymbol{k}$ along the propagation direction:

$$E(\boldsymbol{k}) = k^2/2 + I_p + U_p + k_x U_p/c. \tag{9}$$

The intercycle amplitude following strong-field ionization by an $N$ cycle pulse then reads

$$M_{\boldsymbol{k},0}^{\text{Inter}}(N) = \sum_{n=0}^{N-1} e^{in2\pi \frac{E(\boldsymbol{k})}{\omega}}. \tag{10}$$

Note that the Poisson summation formula, $\sum_{n=-\infty}^{\infty} e^{-2\pi i n x} = \delta(x - n)$, in combination with Eq. (9), gives energy delta functions and ATI peaks when $N$ goes to infinity, i.e., in this limit one obtains the energy in Eq. (3) and the shift in Eq. (4). While the intercycle interference term determines the energy conservation in the long pulse limit, the intracycle dynamics is directly linked to the ionization mechanism. For long wavelengths and high intensity, this mechanism may be tunneling dominated. Since, however, the spectrum may be modeled by the norm squared of a product of inter- and intracycle amplitudes [44–47], any smooth tunneling background will be modulated by strong intercycle interference leading to ATI peaks for the pulses considered below. Recent work uncovered subcycle dynamics by photoelectron holography [47].

In the calculations, which illustrate some consequences of the above discussion for ATI spectra, a typical intensity of $10^{14}$ W/cm$^2$ is used and $N = 10$ cycles are considered for wavelengths $\lambda = 1600$, 2400, 3200, and 6400 nm. For fixed intensity, the increase in $\lambda$ gives rise to an increase in $U_p \sim \lambda^2$ and therefore a range of $\beta_0$ and $\beta_1$ values (see Table I). The target is ground-state atomic hydrogen. The nondipole strong-field-Hamiltonian approach [25] for the SFA ionization

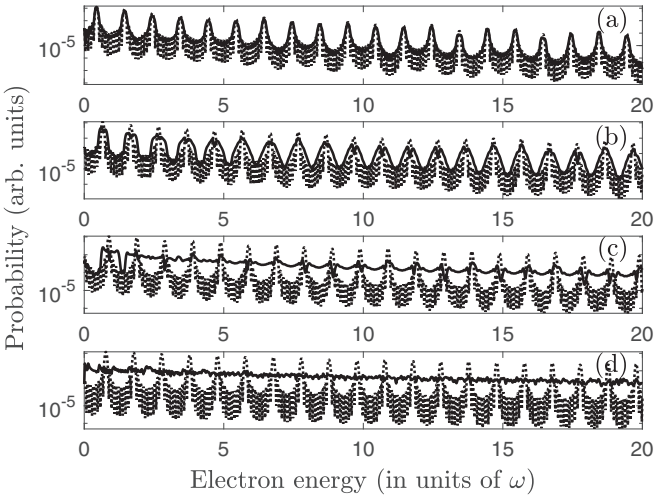


FIG. 1. Disappearance of ATI peaks. ATI spectra from hydrogen for a ten cycle pulse with intensity $10^{14}$ W/cm$^2$ for wavelengths of (a) 1600 nm, (b) 2400 nm, (c) 3200 nm, and (d) 6400 nm. The full curves show results including nondipole effects. The dashed curves show the results within the electric dipole approximation.

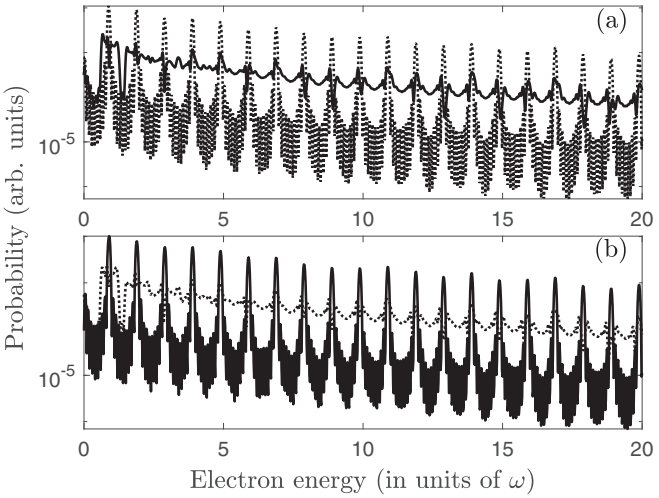


FIG. 2. Reappearance of ATI peaks. (a) ATI spectra from hydrogen for a ten cycle pulse with intensity $10^{14}$ W/cm$^2$ and $\lambda = 3200$ nm. The full curves show results including nondipole effects. The dashed curves show results within the electric dipole approximation. (b) As (a), but with momenta measured with respect to the nondipole-induced shifted center of the energy conserving ATI rings according to Eq. (4).

amplitude is evaluated in the saddle-point approximation including both inter- and intracycle contributions. To this end, the approach taken is the one described in Ref. [45] for the dipole case with the nondipole modifications of the phase and the saddle-point solutions described in Ref. [31]. The PMD is obtained from the norm square of this amplitude. The ATI spectra are obtained by integrating the PMD over electron emission angle for fixed length of the outgoing momentum. Figure 1 shows the photoelectron spectra for the considered wavelengths for the nondipole (full curves) and electric dipole (dashed curve) cases. The figure illustrates that the ATI peaks gradually disappear as $\lambda$ of the driving pulse increases. Indeed, the nondipole ATI spectra at 3200 and 6400 nm are characterized by relatively structureless decreasing curves, and the ATI peaks have disappeared. In contrast, the less accurate electric dipole approximation results show clear ATI peaks at all considered $\lambda$'s. Table I collects the values of the parameters $\beta_0$ and $\beta_1$ for the $\lambda$'s considered in Fig. 1. The values of these parameters support the increase in the nondipole-induced effect seen in Fig. 1 in the sense that a smearing out of the peaks occurs when they attain values around unity.

In the analysis of PMD data, ATI peaks at energies of the different photon absorption channels can be made to reappear if one integrates over the angle of the outgoing electron not with respect to the origin $(k_{x0}, k_{z0}) = (0, 0)$, but with respect to the shifted center $(k_{x0}, k_{z0}) = (-U_p/c, 0)$. The accompanying shifts of the momenta as given by Eqs. (5) and (6) guarantee that the concentric energy conserving rings refer to the shifted center. Figure 2 shows the result for the ATI spectra at 3200 nm when the integration is done with respect to (a) (0,0) and (b) $(-U_p/c, 0)$. After the appropriate emission-angle-dependent modification of the lengths of the outgoing momenta, the data in panel (b) show that ATI peaks reappear in the nondipole data, while the peak structure in the dipole ATI spectrum is washed out by the nondipole shifts. It is worth remembering that the uncertainty in the photon energy scales inversely to the pulse duration, i.e., as $\omega/N$, so keeping the number of cycles, $N$, fixed as the wavelength increases ensures that the ratio of the width of each peak to the distance between the ATI peaks remains $\approx 1/N$, and thus the finite duration of the pulse does in principle not impede the peaks being identified even at 6400 nm. Note that the parameters for the laser used for the results in Fig. 2 are similar to those reported in some experiments [7–10]. An experimental exploration of the present nondipole effects in this wavelength regime therefore seems possible. It is noted that ATI peaks were not clearly observed in the mentioned experiments [7–10]. Their absence is consistent with the present findings. Prior to this paper, a plausible reason for the absence of ATI peaks could be constructed in a picture involving a field-driven rather than a multiphoton-driven ionization mechanism. While the field-driven aspect is certainly important, it is beyond doubt that the quantized nature of the photon energy should show up as soon as there are more than a few cycles in the pulse. The result in Fig. 2 shows how the peaks may be made to reappear by appropriate analysis of momentum resolved data. In an experiment with a pulse containing, say, ten or more cycles and at a fixed long wavelength, say 3200 nm or longer, a procedure to identify the effect would be to perform measurements of the ATI spectrum as a function of laser intensity. At low intensity the magnetic effect is small, $U_p$ is small, and $\beta_0$ and $\beta_1$ are small, and therefore one would observe a few ATI peaks. As the intensity is increased the nondipole effects increase and the smearing out occurs for the reasons discussed above.

It is likewise noted that the shifts of the ATI peaks in the experimental 800-nm work [43] are small and the peaks are still observed, again consistent with the present findings and the small parameter values $\beta_0 \simeq 1.4 \times 10^{-2}$ and $\beta_1(\nu =$

5) $\simeq 4.5 \times 10^{-4}$ under those experimental conditions. It is encouraging that the peaks and shifts of the ATI peaks were detected despite the dependence of $U_p$ on the laser intensity distribution inside the laser beam. Related to experiment, one is led to a general consideration of whether or not it is possible to analyze experimental data such that ATI peaks can be made to reappear. Indeed, if a nondipole PMD is available, the peak structure can be revealed by accounting for the $\theta$-dependent shifts in length of the individual photon absorption channels as described by Eqs. (5) and (6). This reconstruction requires measurement of momenta as vectors. Such vectorial information can be obtained, e.g., in a cold target recoil ion momentum spectroscopy (COLTRIMS) apparatus [42,43]. If, on the other hand, the ATI spectrum is obtained without knowledge of the emission direction, reconstruction of momenta with respect to the shifted center of the ATI rings cannot be performed and the ATI peaks may disappear for intense midinfrared laser pulses.

It is of interest to note that the measure $\beta_1$ depends on the number of photons $\nu$ absorbed above threshold. The right-hand side Eq. (8) increases linearly with $\nu$. This can be exploited to observe nondipole effects at the higher-order ATI peaks even at near-infrared wavelengths. For example at 800 nm and for an intensity of $5 \times 10^{14}$ W/cm$^2$ a value of $\beta_1 = 1$ is obtained for $\nu \simeq 89$ well below the classical cutoff of $10U_p/\omega \simeq 192$. These kind of predictions of trends have been confirmed by calculating spectra for a range of parameters (not shown).

A few remarks on the generality of the present findings are in order. The illustrative calculations were done within a nondipole version of the SFA. The conclusions regarding the disappearance and reappearance of the ATI peak are, however, generally valid. This may be seen in a number of ways. First of all, for pulses containing sufficiently many cycles, the energy relation of Eq. (3) will start describing the momentum positions of the energy-conserving ATI rings. This equation is responsible for the shift of the center of the rings and is therefore responsible for the disappearance of the ATI peaks in the sense discussed above. Secondly, if a Born series in the interaction with the atomic potential is performed in an extension of the SFA to higher order with Volkov propagation between the interactions with the atomic potential, one of the time integrals will give the same energy conservation as the one expressed in Eq. (3); see, e.g., Ref. [48] for a treatment within the dipole approximation. The same conclusion regarding energy conservation is reached using the Coulomb quantum orbit strong-field approximation, which also includes higher-order interactions with the atomic potential [46]. Finally, the predictions of the present approach are consistent with the experimental results at 800 nm [43]. Hence, the energy relation on which the conclusions are based is valid on general grounds, and therefore the predicted effects are insensitive to the specific choice of target.

## III. SUMMARY AND CONCLUSION

The present paper analyzed nondipole ATI spectra. Due to the presence of the nondipole term $k_x U_p/c$ proportional to $k_x$ along the laser propagation direction in the nondipole continuum energy of the outgoing electron, the PMD shifts by $-U_p/c$ in the propagation direction, i.e., by $U_p/c$ opposite to the propagation direction. The intercycle contribution determines the $\boldsymbol{k}$ points with constructive interference and leads to energy conserving rings in the limit of many cycles. For intense midinfrared laser pulses, it was shown how the expected peaks in the ATI spectrum may disappear due to nondipole effects, but can be made to reappear when the nondipole-induced shift of the center of the ATI rings is taken into account in the analysis of the photoelectron momenta. These emission-angle-dependent momentum modifications are useful in the analysis of experimental data with intense midinfrared lasers, and allow a recovery of clear ATI peaks.

This work was supported by the Independent Research Fund Denmark (Grants No. 9040-00001B and No. 1026-00040B).

[1] C. T. L. Smeenk, L. Arissian, B. Zhou, A. Mysyrowicz, D. M. Villeneuve, A. Staudte, and P. B. Corkum, Partitioning of the Linear Photon Momentum in Multiphoton Ionization, Phys. Rev. Lett. **106**, 193002 (2011).

[2] N. Haram, I. Ivanov, H. Xu, K. T. Kim, A. Atia-tul Noor, U. S. Sainadh, R. D. Glover, D. Chetty, I. V. Litvinyuk, and R. T. Sang, Relativistic Nondipole Effects in Strong-Field Atomic Ionization at Moderate Intensities, Phys. Rev. Lett. **123**, 093201 (2019).

[3] A. Hartung, S. Eckart, S. Brennecke, J. Rist, D. Trabert, K. Fehre, M. Richter, H. Sann, S. Zeller, K. Henrichs, G. Kastirke, J. Hoehl, A. Kalinin, M. S. Schöffler, T. Jahnke, L. Ph. H. Schmidt, M. Lein, M. Kunitski, and R. Dörner, Magnetic fields alter strong-field ionization, Nat. Phys. **15**, 1222 (2019).

[4] A. Hartung, S. Brennecke, K. Lin, D. Trabert, K. Fehre, J. Rist, M. S. Schöffler, T. Jahnke, L. Ph. H. Schmidt, M. Kunitski, M. Lein, R. Dörner, and S. Eckart, Electric Nondipole Effect in Strong-Field Ionization, Phys. Rev. Lett. **126**, 053202 (2021).

[5] N. Haram, H. Xu, I. Ivanov, D. Chetty, I. Litvinyuk, and R. T. Sang, Strong-field ionization of argon: Electron momentum spectra and nondipole effects, Phys. Rev. A **105**, 023522 (2022).

[6] K. Lin, S. Brennecke, H. Ni, X. Chen, A. Hartung, D. Trabert, K. Fehre, J. Rist, X.-M. Tong, J. Burgdörfer, L. Ph. H. Schmidt, M. S. Schöffler, T. Jahnke, M. Kunitski, F. He, M. Lein, S. Eckart, and R. Dörner, Magnetic-Field Effect in High-Order Above-Threshold Ionization, Phys. Rev. Lett. **128**, 023201 (2022).

[7] A. Ludwig, J. Maurer, B. W. Mayer, C. R. Phillips, L. Gallmann, and U. Keller, Breakdown of the Dipole Approximation in Strong-Field Ionization, Phys. Rev. Lett. **113**, 243001 (2014).

[8] J. Maurer, B. Willenberg, J. Daněk, B. W. Mayer, C. R. Phillips, L. Gallmann, M. Klaiber, K. Z. Hatsagortsyan, C. H. Keitel, and U. Keller, Probing the ionization wave packet and recollision dynamics with an elliptically polarized strong laser field in the nondipole regime, Phys. Rev. A **97**, 013404 (2018).

[9] J. Daněk, M. Klaiber, K. Z. Hatsagortsyan, C. H. Keitel, B. Willenberg, J. Maurer, B. W. Mayer, C. R. Phillips, L. Gallmann, and U. Keller, Interplay between coulomb-focusing and non-dipole effects in strong-field ionization with elliptical polarization, J. Phys. B: At., Mol. Opt. Phys. **51**, 114001 (2018).

[10] B. Willenberg, J. Maurer, B. W. Mayer, and U. Keller, Subcycle time resolution of multi-photon momentum transfer in strong-field ionization, Nat. Commun. **10**, 5548 (2019).

[11] M. Klaiber, K. Z. Hatsagortsyan, and C. H. Keitel, Above-threshold ionization beyond the dipole approximation, Phys. Rev. A **71**, 033408 (2005).

[12] M. Klaiber, E. Yakaboylu, H. Bauke, K. Z. Hatsagortsyan, and C. H. Keitel, Under-the-Barrier Dynamics in Laser-Induced Relativistic Tunneling, Phys. Rev. Lett. **110**, 153004 (2013).

[13] E. Yakaboylu, M. Klaiber, H. Bauke, K. Z. Hatsagortsyan, and C. H. Keitel, Relativistic features and time delay of laser-induced tunnel ionization, Phys. Rev. A **88**, 063421 (2013).

[14] S. Chelkowski, A. D. Bandrauk, and P. B. Corkum, Photon Momentum Sharing between an Electron and an Ion in Photoionization: From One-Photon (Photoelectric Effect) to Multiphoton Absorption, Phys. Rev. Lett. **113**, 263005 (2014).

[15] S. Chelkowski, A. D. Bandrauk, and P. B. Corkum, Photon-momentum transfer in multiphoton ionization and in time-resolved holography with photoelectrons, Phys. Rev. A **92**, 051401(R) (2015).

[16] K. Krajewska and J. Z. Kamiński, Radiation pressure in strong-field-approximation theory: Retardation and recoil corrections, Phys. Rev. A **92**, 043419 (2015).

[17] S. Chelkowski and A. D. Bandrauk, Photon momentum transfer in photoionisation: Unexpected breakdown of the dipole approximation, Mol. Phys. **115**, 1971 (2017).

[18] P.-L. He, D. Lao, and F. He, Strong Field Theories beyond Dipole Approximations in Nonrelativistic Regimes, Phys. Rev. Lett. **118**, 163203 (2017).

[19] S. Brennecke and M. Lein, High-order above-threshold ionization beyond the electric dipole approximation, J. Phys. B: At., Mol. Opt. Phys. **51**, 094005 (2018).

[20] S. Brennecke and M. Lein, High-order above-threshold ionization beyond the electric dipole approximation: Dependence on the atomic and molecular structure, Phys. Rev. A **98**, 063414 (2018).

[21] S. Chelkowski and A. D. Bandrauk, Photon-momentum transfer in molecular photoionization, Phys. Rev. A **97**, 053401 (2018).

[22] S. Brennecke and M. Lein, Strong-field photoelectron holography beyond the electric dipole approximation: A semiclassical analysis, Phys. Rev. A **100**, 023413 (2019).

[23] B. Böning, W. Paufler, and S. Fritzsche, Nondipole strong-field approximation for spatially structured laser fields, Phys. Rev. A **99**, 053404 (2019).

[24] B. Willenberg, J. Maurer, U. Keller, J. Daněk, M. Klaiber, N. Teeny, K. Z. Hatsagortsyan, and C. H. Keitel, Holographic interferences in strong-field ionization beyond the dipole approximation: The influence of the peak and focal-volume-averaged laser intensities, Phys. Rev. A **100**, 033417 (2019).

[25] S. V. B. Jensen, M. M. Lund, and L. B. Madsen, Nondipole strong-field-approximation hamiltonian, Phys. Rev. A **101**, 043408 (2020).

[26] H. Ni, S. Brennecke, X. Gao, P.-L. He, S. Donsa, I. Březinová, F. He, J. Wu, M. Lein, X.-M. Tong, and J. Burgdörfer, Theory of Subcycle Linear Momentum Transfer in Strong-Field Tunneling Ionization, Phys. Rev. Lett. **125**, 073202 (2020).

[27] S. Brennecke and M. Lein, Nondipole modification of the ac stark effect in above-threshold ionization, Phys. Rev. A **104**, L021104 (2021).

[28] M. M. Lund and L. B. Madsen, Nondipole photoelectron momentum shifts in strong-field ionization with mid-infrared laser pulses of long duration, J. Phys. B: At., Mol. Opt. Phys. **54**, 165602 (2021).

[29] P.-L. He, K. Z. Hatsagortsyan, and C. H. Keitel, Nondipole Time Delay and Double-Slit Interference in Tunneling Ionization, Phys. Rev. Lett. **128**, 183201 (2022).

[30] M. Klaiber, K. Z. Hatsagortsyan, and C. H. Keitel, Subcycle time-resolved nondipole dynamics in tunneling ionization, Phys. Rev. A **105**, 053107 (2022).

[31] L. B. Madsen, Nondipole effects in tunneling ionization by intense laser pulses, Phys. Rev. A **105**, 043107 (2022).

[32] J. Liang, Y. Zhou, W.-C. Jiang, M. Yu, M. Li, and P. Lu, Zeeman effect in strong-field ionization, Phys. Rev. A **105**, 043112 (2022).

[33] R. Kahvedžić and S. Gräfe, Strong-field approximation with leading-order nondipole corrections, Phys. Rev. A **105**, 063102 (2022).

[34] H. R. Reiss, Relativistic strong-field photoionization, J. Opt. Soc. Am. B **7**, 574 (1990).

[35] H. R. Reiss, Limits on Tunneling Theories of Strong-Field Ionization, Phys. Rev. Lett. **101**, 043002 (2008).

[36] H. R. Reiss, Relativistic effects in nonrelativistic ionization, Phys. Rev. A **87**, 033421 (2013).

[37] H. R. Reiss, The tunnelling model of laser-induced ionization and its failure at low frequencies, J. Phys. B: At., Mol. Opt. Phys. **47**, 204006 (2014).

[38] M.-X. Wang, S.-G. Chen, H. Liang, and L.-Y. Peng, Review on non-dipole effects in ionization and harmonic generation of atoms and molecules, Chin. Phys. B **29**, 013302 (2020).

[39] N. Haram, R. T. Sang, and I. V. Litvinyuk, Transverse electron momentum distributions in strong-field ionization: nondipole and coulomb focusing effects, J. Phys. B: At., Mol. Opt. Phys. **53**, 154005 (2020).

[40] J. Maurer and U. Keller, Ionization in intense laser fields beyond the electric dipole approximation: Concepts, methods, achievements and future directions, J. Phys. B: At., Mol. Opt. Phys. **54**, 094001 (2021).

[41] R. R. Freeman, P. H. Bucksbaum, W. E. Cooke, G. Gibson, T. J. Mcllrath, and L. D. van Woerkom, in *Atoms in Intense Laser Fields*, edited by M. Gavrila (Academic, New York, 1992).

[42] C. J. Joachain, N. J. Kylstra, and R. M. Potvliege, *Atoms in Intense Laser Fields* (Cambridge University, New York, 2011).

[43] K. Lin, S. Eckart, A. Hartung, D. Trabert, K. Fehre, J. Rist, L. Ph. H. Schmidt, M. S. Schöffler, T. Jahnke, M. Kunitski, and R. Dörner, Photoelectron energy peaks shift against the radiation pressure in strong-field ionization, Sci. Adv. **8**, eabn7386 (2022).

[44] D. G. Arbó, K. L. Ishikawa, K. Schiessl, E. Persson, and J. Burgdörfer, Intracycle and intercycle interferences in above-

threshold ionization: The time grating, Phys. Rev. A **81**, 021403(R) (2010).

[45] D. G. Arbó, K. L. Ishikawa, E. Persson, and J. Burgdörfer, Doubly differential diffraction at a time grating in above-threshold ionization: Intracycle and intercycle interferences, Nucl. Instrum. Methods Phys. Res., Sect. B **279**, 24 (2012).

[46] A. S. Maxwell, A. Al-Jawahiry, T. Das, and C. F. de Morisson Faria, Coulomb-corrected quantum interference in above-threshold ionization: Working towards multitrajectory electron holography, Phys. Rev. A **96**, 023420 (2017).

[47] N. Werby, A. S. Maxwell, R. Forbes, P. H. Bucksbaum, and C. F. de Morisson Faria, Dissecting subcycle interference in photoelectron holography, Phys. Rev. A **104**, 013109 (2021).

[48] A. Lohr, M. Kleber, R. Kopold, and W. Becker, Above-threshold ionization in the tunneling regime, Phys. Rev. A **55**, R4003 (1997).